Intelligent Oncology 1 (2025) 7–16

Contents lists available at ScienceDirect

Intelligent Oncology

journal homepage: www.keaipublishing.com/en/intonc/

Full Length Article

Discovery of novel EGFR and BRAF inhibitors by machine learning approach

Hailong Zhang[a,*], Henry H.Y. Tong[a,b]

[a] Faculty of Applied Sciences, Macao Polytechnic University, Macao Special Administrative Region 999078, China
[b] Faculty of Health Sciences and Sports, Macao Polytechnic University, Macao Special Administrative Region 999078, China

ARTICLE INFO

Keywords:
Cancer
EGFR
BRAF
Machine learning
Artificial intelligence

ABSTRACT

Background: In the pharmaceutical industry, epidermal growth factor receptor (EGFR) and B-Raf proto-oncogene, serine/threonine kinase (BRAF) are the primary targets for targeted cancer therapy.
Objective: This study aimed to develop novel models for predicting the bioactivity of EGFR and BRAF inhibitors and to uncover critical substructural groups for EGFR and BRAF targets.
Method: K-nearest neighbor, Gaussian naive Bayes, random forest (RF), decision tree, and support vector machine models were utilized to develop classifiers for EGFR and BRAF inhibitors. In addition, the critical functional groups of these inhibitors were analyzed, and molecular docking was performed.
Results: The RF model was found to be the preferred choice for predicting the bioactivity of EGFR and BRAF inhibitors. The RF model for BRAF had an accuracy and area under the curve (AUC) of 93% and 0.96, respectively, and the RF model for EGFR had an accuracy and AUC of 90% and 0.96, respectively. The results of this study show the importance of properly increasing chlorine or fluorine in inhibitors of BRAF or EGFR. Moreover, the EGFR and BRAF inhibitors exhibited the same halogen selection priority of fluorine > chlorine > bromine.
Conclusion: The present study develops novel models for predicting the bioactivity of EGFR and BRAF inhibitors. The hydrogen bond formation is a key factor for influencing the selection priority of fluorine > chlorine > bromine.

1. Introduction

Lung cancer is a leading cause of death worldwide, accounting for more than 1.8 million deaths annually.[1] Small cell lung cancer and non-small cell lung cancer are two major histological types of lung cancer,[2–4] and adenocarcinoma mainly occurs in non-small cell lung cancer.[5] In patients with lung cancer, targeted therapy has been demonstrated to be more beneficial and to produce longer survival times than chemotherapy.[6–9] In recent years, epidermal growth factor receptor (EGFR) and B-Raf proto-oncogene, serine/threonine kinase (BRAF) have become attractive targets for lung cancer therapy.

As a member protein of the ErbB receptor family,[10] EGFR has intracellular, extracellular, and transmembrane domains. The intracellular domain of EGFR can bind to small molecular inhibitors.[11] EGFR mutations occurring in the tyrosine kinase domain can result in constitutive EGFR signaling and cancer. The L858R mutation occurring in the EGFR protein is sensitive to targeted EGFR inhibitors, such as gefitinib and erlotinib.[12–16]

* Corresponding author.
E-mail address: p2314575@mpu.edu.mo (H. Zhang).

https://doi.org/10.1016/j.intonc.2024.10.001
Received 30 March 2024; Received in revised form 20 September 2024; Accepted 11 October 2024
Available online 20 December 2024
2950-2616/© 2025 The Author(s). Publishing services by Elsevier B.V. on behalf of KeAi Communications Co. Ltd. This is an open access article under the CC BY license (http://creativecommons.org/licenses/by/4.0/).

Targeted lung cancer therapy has been demonstrated to control symptoms, increase quality of life, and generate higher responses than conventional chemotherapy. However, an increase in resistance to the drugs involved in these therapies has negatively impacted their effectiveness, with some lung cancer patients failing to have a positive response. Thus, the development of novel inhibitor therapies is needed.

At present, EGFR mutations T790M and C797S are a major problem in cancer targeted therapy because they promote drug resistance in targeted therapies employing the inhibitors gefitinib or erlotinib.[17,18] Therefore, novel targeted drugs that can neutralize the effects of T790M and C797S mutations are needed.

As a type of ser-thr protein kinase, BRAF is essential to the Mitogen-activated protein kinase, which affects cell division and differentiation.[19–21] After being found in melanomas,[22,23] the BRAF V600E mutation was identified in patients with lung cancer.[24] Both EGFR and BRAF proteins are engaged in cellular proliferation, division, and differentiation.[25–28]

An effective strategy for resolving the issue of targeted drug therapy resistance in lung cancer patients is to focus on the discovery of novel EGFR inhibitors based on the L858R, T790M, and C797S mutations and downstream BRAF inhibitors, thereby simultaneously inhibiting EGFR and BRAF signaling. In this study, novel models were developed to predict the bioactivities of EGFR and BRAF inhibitors, and to analyze the key functional groups and substructures of these inhibitors. To the best of our knowledge, this study is the first to uncover the critical substructural features of EGFR and BRAF inhibitors.

2. Materials and methods

2.1. Data preparation

In this research, two datasets of EGFR and BRAF target inhibitors were obtained from the following databases: ChEMBL, Drugbank, and bindingdb.[29,30] Because the Simplified Molecular Input-Line Entry System (SMILES) may have duplication or invalidation in raw data, we used a cleaning program to exclude duplicated, null, or invalid molecules SMILES from the raw data. Subsequently, a total of 740 molecules of EGFR inhibitors and 2,866 molecules of BRAF inhibitors were obtained. These validated molecules and their IC50 values were used to construct two datasets.

The activity thresholds of the IC50 of the EGFR and BRAF inhibitors were less than 60 nM, which indicates that an inhibitor with an IC50 value equal to or more than 60 nM was categorized into the inactive group. The development scheme in this research is presented in Figure 1. The EGFR and BRAF inhibitor datasets were each divided into training (80%) and test (20%) subsets for use in

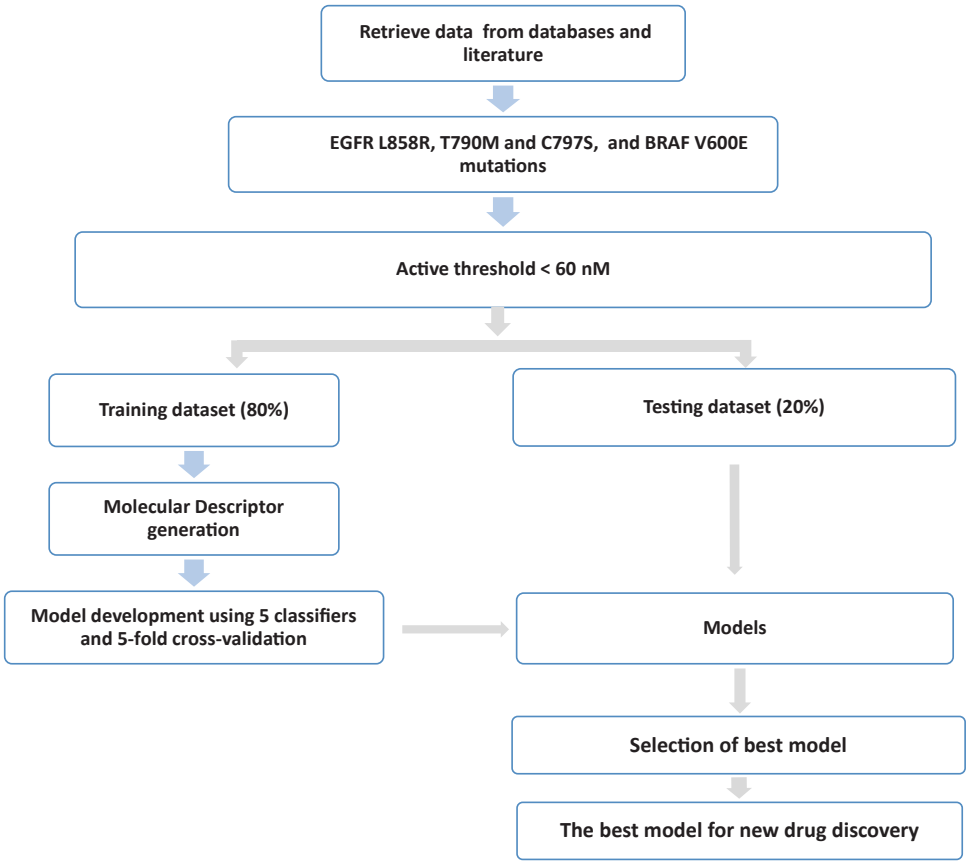


Figure 1. Model development scheme.

model development. For the EGFR inhibitor dataset, 358 were placed in the active group and 382 in the inactive group. For the BRAF inhibitor dataset, 2,117 molecules were placed in the active group and 749 in the inactive group.

2.2. Molecular descriptors

Molecular descriptors are numerical representations of chemical information obtained through mathematical processes. In this study, the ECFP4 molecular fingerprints of the inhibitors and the RDKit tool were used to calculate the molecular descriptors.

2.3. Model development and evaluation

The EGFR inhibitors of L858R, T790M, and C797S mutations and the BRAF target inhibitors of V600E mutation were used to construct the datasets. Five machine learning–based classification models were developed, and their performance in predicting EGFR and BRAF inhibitors was evaluated.

First, k-nearest neighbor (KNN) and Gaussian naive Bayes (GNB) algorithms were adopted for developing the model. GNB is a probabilistic classifier based on applying Bayes' theorem with strong independence assumptions between the features. To improve performance, more sophisticated machine learning algorithms, including random forest (RF), decision tree (DT), and support vector machine (SVM), were subsequently utilized. DT is a tree-based model that recursively splits a dataset into subsets based on certain conditions, and SVM is a machine learning algorithm grounded in statistical learning theory that is used to find the optimal hyperplane, which maximizes the margin between classes. The RF algorithm, introduced by Leo Breiman in 2001,[31] is based on ensemble learning and combines multiple decision trees to generate a more accurate and robust prediction.

The feature selections of each model were determined through steps transforming the raw data into a format suitable for input into a machine learning algorithm. The features of each model were determined by converting SMILES strings into Mol objects using the RDKit library. The Mol objects were then employed to calculate extended circular fingerprints (ECFPs), thereby encoding structural information as binary vectors. The compounds' activity of IC50 was determined using a predefined threshold as described in Section 2.1, resulting in a column indicating the group to which the inhibitor belonged: active or inactive.

The metrics of sensitivity (SE), specificity (SP), harmonic mean (F1), and Matthews correlation coefficient (MCC) were employed to evaluate the models. The receiver operating characteristic (ROC), area under the curve (AUC), and accuracy (ACC) were also adopted for model evaluation. In addition, 5-fold cross-validation was applied to the training group.

2.4. Functional group and substructural analysis

In addition to effective prediction models, a program was developed to conduct functional group or substructural analysis and to compare the frequency of functional groups in the active and inactive groups of the BRAF and EGFR inhibitor datasets.

The number of key functional groups or substructures in the active and inactive groups was analyzed for both inhibitors. The average frequency of substructures in the active group was calculated by dividing the total number of active groups. The average frequency of substructures in the inactive group was calculated using the same method. The key functional groups and substructures enhancing bioactivity were identified by comparing the frequency of substructures in the active and inactive groups. To identify key substructural rings in the inhibitor structures, the number of 3-ring to 7-ring substructures in the EGFR and BRAF inhibitor datasets was calculated using the same method.

2.5. Molecular docking

Protein and ligand docking were carried out using this molecule against EGFR and BRAF target proteins in a molecular operating environment system. The cocrystal structures of the EGFR and BRAF proteins were collected from the protein data bank. The water and original ligand small molecules were removed in preparation for docking.

3. Results

3.1. Classifiation models

In this study, five machine learning algorithms—RF, SVM, KNN, GNB, and DT—were utilized to develop predictive models for EGFR and BRAF inhibitors. For the BRAF target, the accuracy of the RF, SVM, KNN, GNB, and DT models was 93%, 91%, 92%, 66%, and 91%, respectively. The AUC of the BRAF-target RF model was 0.96. The ROCs of the RF and SVM models of the BRAF target are shown in Figure 2a and 2b. Results of the DeLong test showed significant differences in the AUC values of the DT/GNB and RF models ($P < 0.05$). However, no significant differences were observed between the AUC values of the SVM/KNN and RF models ($P > 0.05$). The RF model was preferred for predicting the bioactivity of BRAF inhibitors (Table 1).

For EGFR target, the accuracy of RF, SVM, KNN, GNB, and DT was 90%, 89%, 88%, 84%, and 86%, respectively (Table 2). The AUC of the EGFR-targeting RF model was 0.96. The ROCs for the EGFR-targeting RF and SVM models are shown in Figure 2c and 2d. Results of the DeLong Test showed significant differences in AUC values between the DT/GNB and RF models ($P < 0.05$). However, no significant differences in AUC were observed between the SVM/KNN and RF models ($P > 0.05$). Nevertheless, the RF model was

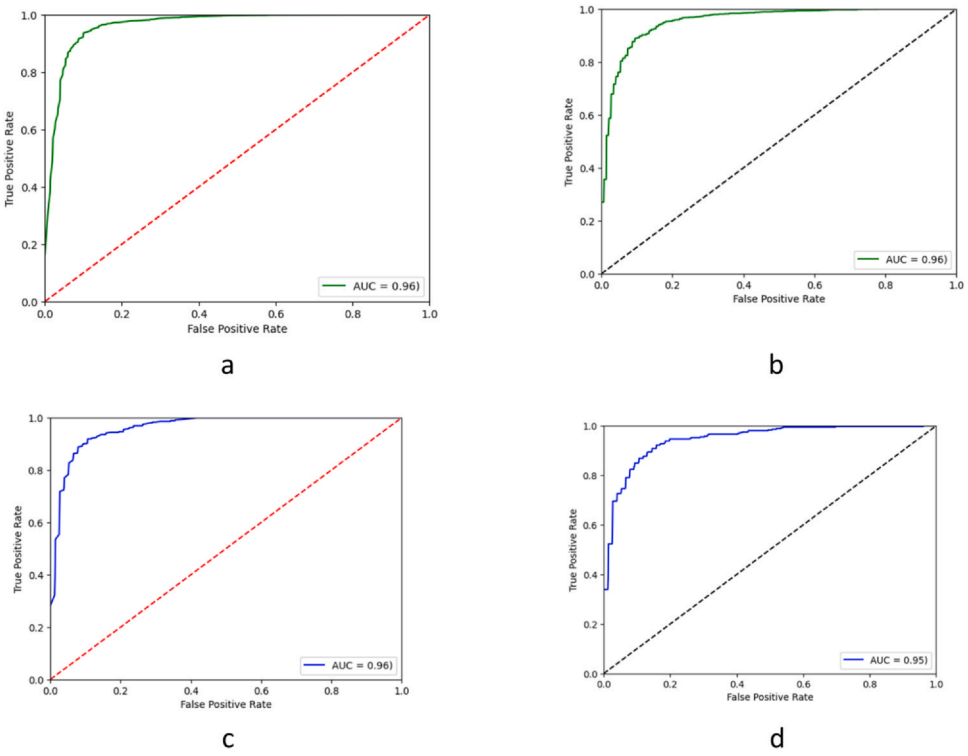


Figure 2. ROC curves. **a**: BRAF target: ROC curve of RF model. **b**: BRAF target: ROC curve of SVM model. **c**: EGFR target: ROC curve of RF model. **d**: EGFR target: ROC curve of SVM model.

Table 1
Performance of different models for BRAF target.

Model	Accuracy	Specificity	Sensitivity	F1	MCC	AUC
RF	0.93	0.82	0.97	0.96	0.82	0.96
SVM	0.91	0.71	0.97	0.94	0.75	0.96
KNN	0.92	0.78	0.97	0.95	0.78	0.93
GNB	0.66	0.88	0.59	0.72	0.41	0.87
DT	0.91	0.83	0.94	0.94	0.77	0.89

Table 2
Performance of different models for EGFR target.

Model	Accuracy	Specificity	Sensitivity	F1	MCC	AUC
RF	0.90	0.88	0.93	0.90	0.81	0.96
SVM	0.89	0.89	0.89	0.88	0.77	0.95
KNN	0.88	0.86	0.90	0.88	0.76	0.93
GNB	0.84	0.82	0.87	0.84	0.69	0.85
DT	0.86	0.86	0.86	0.86	0.72	0.85

found to perform better than the SVM and KNN models in terms of the comprehensive assessment of F1, MCC, and AUC. Thus, the RF model was shown to be more effective predicting the bioactivity of EGFR inhibitors.

For EGFR target, the accuracy of the RF model was found to be superior to that of the KNN model, a finding smiliar to a previous study[32] Although the mutation sites and data of EGFR are different, it may provide a reference. The RF model was identified as most suitable for predicting the bioactivity of both BRAF and EGFR inhibitors. However, it was more accurate at predicting the bioactivity of BRAF inhibitors. This may be due to the various structures of the EGFR inhibitors, since three mutations (L858R, T790M, and C797S) were used to establish the models, whereas the structures of the BRAF inhibitors were more unified, with the model using only one mutation (V600E). Consequently, models for the BRAF inhibitors showed higher accuracy than those for the EGFR inhibitors.

3.2. Resluts of functional group and substructural analysis

This study also developed a program for comparing the active and inactive substructural groups of BRAF and EGFR inhibitors. The findings indicate that the amount of chlorine and fluorine in the active BRAF group was greater than in the inactive group, which suggests that chlorine and fluorine are critical factors for BRAF inhibitors. However, bromine was rarely found in either the active or inactive groups, suggesting that chlorine and fluorine cannot be replaced by bromine in the structures of BRAF inhibitors. Thus, the selection priority of these three elements in the chemical structure of BRAF-targeting inhibitors is fluorine > chlorine > bromine. Moreover, the frequency of the substructure of C≡N in the active group was approximately twice as high as that in the inactive group, and the frequency of the functional group of C═O was higher in the active group than in the inactive group (Figure 3a).

Conversely, in the EGFR-targeting inhibitors, the frequency of the substructures C≡N and C═O was lower in the active group than in the inactive group. Additionally, phosphorus was not found in the structures of the BRAF inhibitors but was found in the structures of the EGFR inhibitors (Figure 3b). Similarly, the frequency of the group of NH in the structures of the EGFR inhibitors was higher than that of the BRAF inhibitors.

Furthermore, 3- to 7-ring structural features in the EGFR and BRAF inhibitors were identified in this research, with 5- and 6-ring structures being the most prolific (Figure 4a). The frequency of 3-, 4-, and 7-ring structures ranged from 2% to 14% (Figure 4a), with a 4-ring structure with three carbons and one nitrogen having the same frequency of approximately 2.8% in both EGFR and BRAF inhibitors. It was determined that the optimum EGFR inhibitor structure contains one 5-ring, three or four 6-rings, and zero to two 6-rings with one or two nitrogen atoms, whereas the optimum BRAF inhibitor structure contains zero or one 5-ring, three or four 6-rings, and one or two 6-rings containing one or two nitrogen atoms (Table 3).

3.3. Molecular docking results

The molecule LMEB-1 (Figure 5a) was employed to perform molecular docking based on the substructural features of the inhibitors. The molecule exhibited good docking scores for both EGFR and BRAF, indicating the molecule's ability to bind to these two targets. The molecule showed docking scores of −6.79 and −8.13 with EGFR and BRAF, respectively.

Two hydrogen bonds were observed between the molecule and the EGFR target, with MET790 and LYS745 engaged in this interaction (Figure 5b and 5c and Table 4). Three amino acid residues—SER536, PHE595, and VAL471—were observed to be engaged in the interaction between the BRAF target protein and the molecule, and two hydrogen bonds were observed between the molecule and the amino acid residues PHE595 and SER536 (Figure 5d and 5e and Table 4). Moreover, the molecule was found to have more than one special interaction of pi-H with the BRAF target protein.

4. Discussion

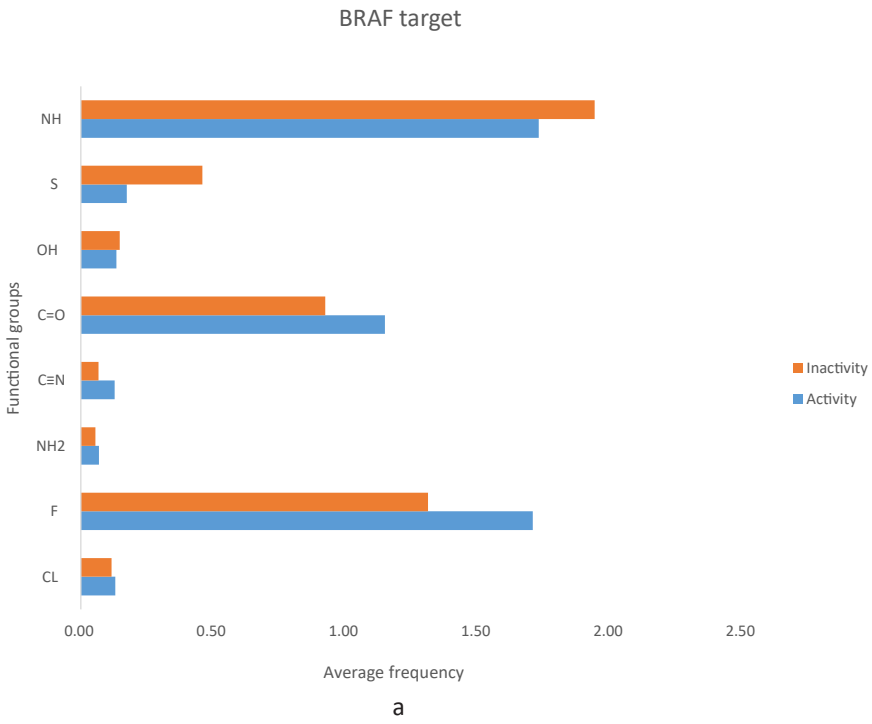
Currently, the drug-resistant EGFR mutations T790M and C797S are a major problem for targeted cancer therapy. Thus, the development of novel drugs targeting these mutations is critical to further improving targeted therapy for cancer patients. The predictive models developed in this study are valuable tools for the discovery of antiresistance EGFR inhibitors. We also established predictive models for BRAF inhibitors, providing treatment options for cancer patients. Besides, we developed and compared the performance of the RF, SVM, KNN, GNB, and DT predictive models in EGFR and BRAF inhibitors.

The accuracy ranking of the five algorithms in the BRAF model was similar to that of the EGFR model, which may indicate that BRAF and EGFR inhibitors show much similarity. However, the DT model of EGFR target was less accurate than the DT model of BRAF target, with the KNN algorithm having a similar pattern. These results may suggest that the DT and KNN algorithms are more suitable for single mutation target model development. The GNB algorithm had the lowest accuracy, particularly in relation to the BRAF model, which may imply that the GNB model is inappropriate for involving these types of inhibitors. The results also demonstrate that it may be helpful to obtain a higher accuracy by comparing more algorithms, which may be a limitation of the present study.

Moreover, the elements of chlorine and fluorine were in higher frequency in the active group than in the inactive group of EGFR inhibitors and exhibited a selecting priority of fluorine > chlorine > bromine. This selection priority was similar to that of the BRAF inhibitors. In contrast to inhibitors of BRAF target, the bromine occasionally appeared to replace fluorine or chlorine in EGFR inhibitor structures. However, the elements of fluorine and chlorine were irreplaceable by bromine in the inhibitor structures of the BRAF target. Bromine is not a good option for use in BRAF-based anticancer drugs. However, bromine is often adopted in the treatment of respiratory disease. For example, the drug ambroxol hydrochloride (C13H19Br2ClN2O) contains bromine and is used to treat respiratory diseases associated with excessive mucus.[33] Similarly, bromhexine hydrochloride contains bromine and is used to decrease the viscosity of mucus in the airway, thereby easing the difficulty breathing and discomfort associated with various respiratory diseases.[34] As a result, the phenomenon of using bromine may be related to the type of disease being treated.

Notably, an ideal inhibitor molecule should have one fluorine, three 6-rings, one 6-ring containing one nitrogen, one 5-ring, one group of C═O, two groups of NH, and 5 nitrogens (Table 5). Although chlorine is lower in the selecting priority than fluorine, chlorine is acceptable for both EGFR and BRAF inhibitors.

The importance of fluorine or chlorine was interpreted by molecular docking analysis. Because fluorine and chlorine form hydrogen bonds with the amino acids of the targeted proteins, they play a critical role in the molecular structure. Given that fluorine forms hydrogen bonds easily while bromine does not, the selecting priority for the EGFR/BRAF inhibitors should be fluorine > chlorine > bromine. The molecule LMEB-1 was able to bind with both EGFR and BRAF. However, based on docking scores and binding bonds, the molecule showed more affinity for the BRAF than for EGFR.



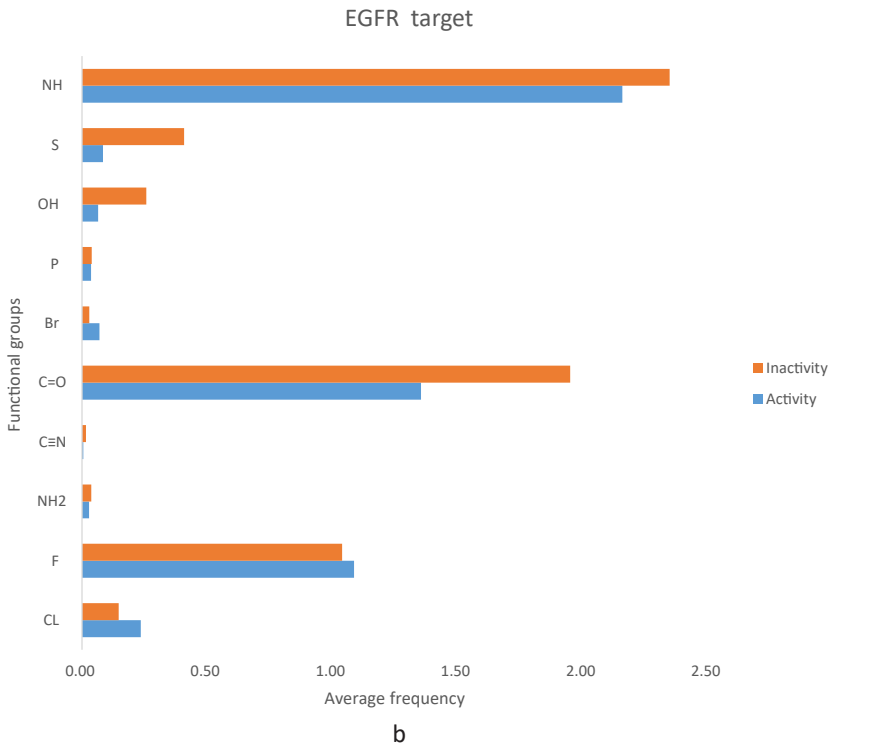


Figure 3. Average frequency of functional groups between active group and inactive group. **a**: Average frequency of functional groups between active group and inactive group for the inhibitors of BRAF target. **b**: Average frequency of functional groups between active group and inactive group for the inhibitors of EGFR target.

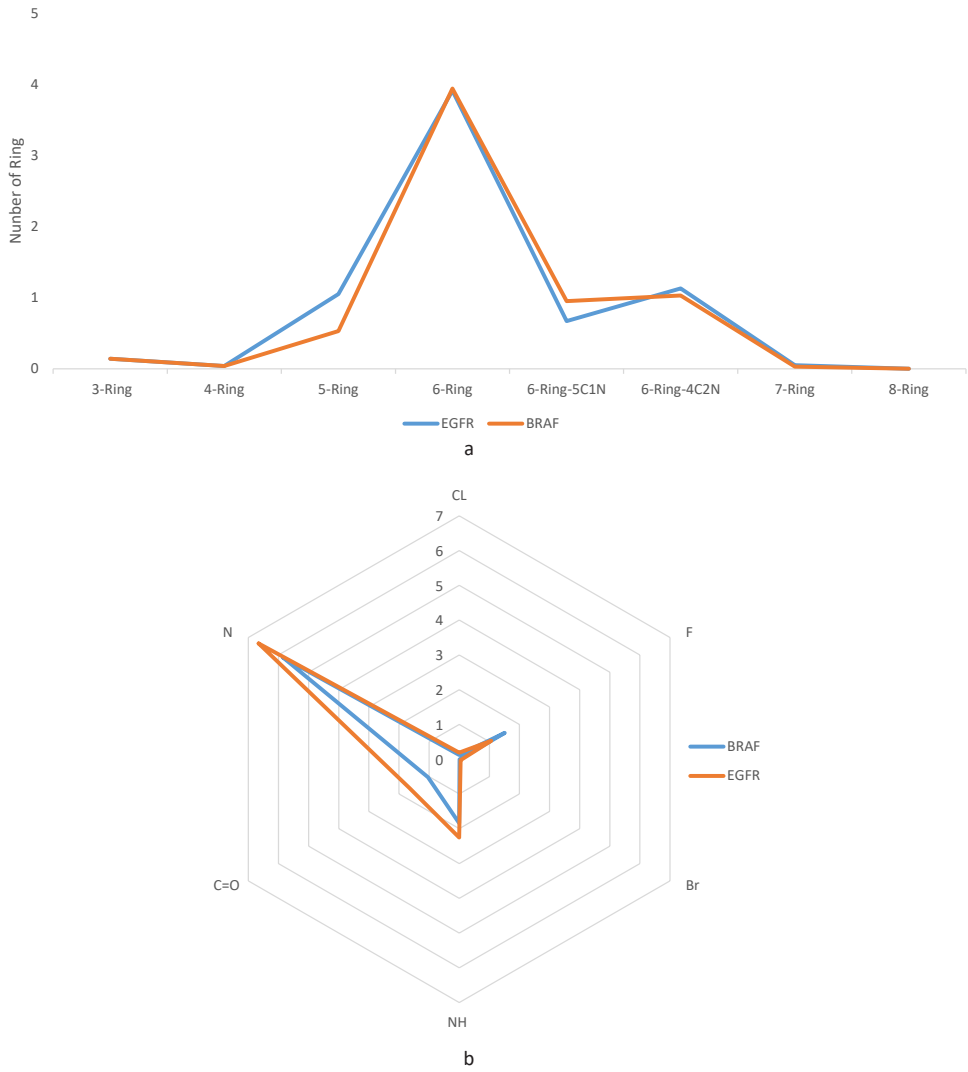
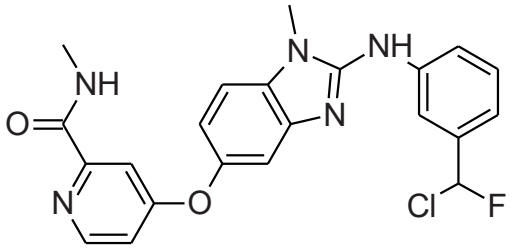


Figure 4. The key substructural groups. **a**: The key substructural ring of EGFR and BRAF target inhibitors. **b**: Radar map of key functional groups of EGFR and BRAF target inhibitors.

Table 3
Key substructural features for inhibitors of EGFR and BRAF targets.

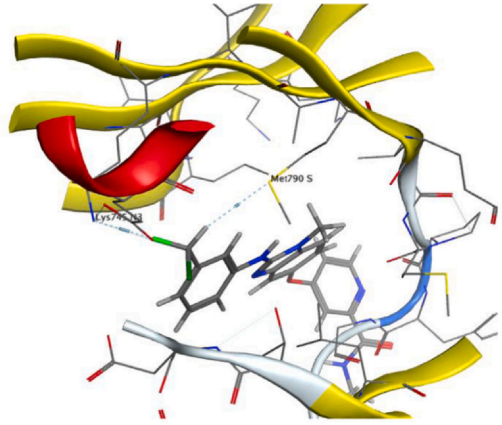
Target	Number of 5-Ring	Number of 6-Ring	Number of 6-Ring (5C1N and 4C2N)
EGFR	1	3–4	0–2
BRAF	0–1	3–4	1–2

The development of multitarget drugs is a promising trend in cancer therapy.[35] In the present study, functional and substructural analyses of BRAF and EGFR inhibitors revealed critical substructural features. First, it is important to enhance bioactivity by increasing the amount of chlorine or fluorine in the structures of BRAF and EGFR inhibitors. However, the functional group C6N should be used with caution since it showed inverse effects on the active groups of the BRAF and EGFR inhibitors. Also, bromine use should be carefully adopted since it was rarely found in the BRAF inhibitors. Second, the number of NH groups should be 2 or 3, and the number of fluorine should be 1 or 2, aligning with the common ranges in the structures of both BRAF and EGFR inhibitors (Table 6 and Figure 4b). Third, the optimum EGFR- or BRAF-inhibitor structure should contain zero or one 5-ring, three or four 6-rings, and one or two 6-rings containing zero to two nitrogen atoms (Table 3).

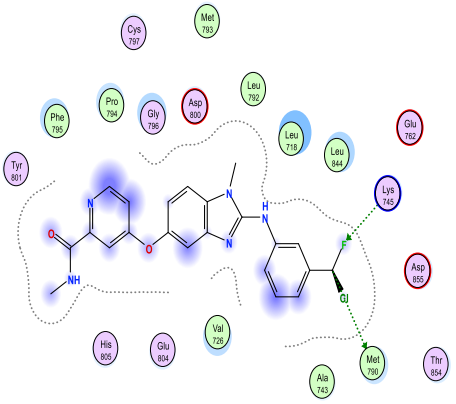


LMEB-1

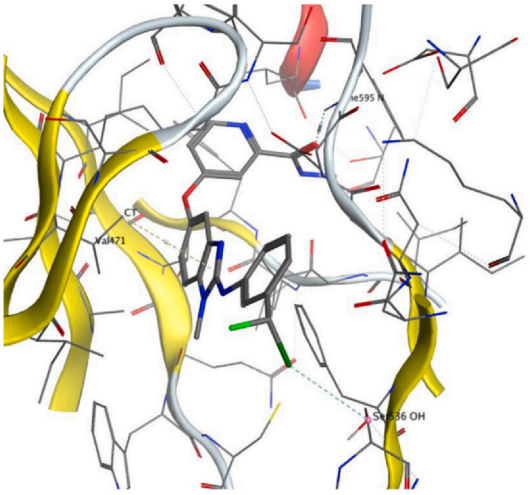
a



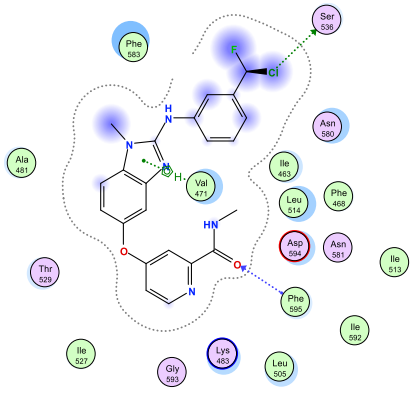
b



c



d



e

Figure 5. Molecular docking. **a**: Chemical structure of molecule LMEB-1. **b**: Snapshots of docking pose of the compound interacting with EGFR protein. **c**: Interaction details between the compound and EGFR protein. **d**: Snapshots of docking pose of the compound interacting with BRAF protein. **e**: Interaction details between the compound and BRAF protein.

Table 4
Bonding characterization of compound interacting with EGFR and BRAF targets.

Target	Bonding interaction	Bond type	Distance	E (kcal/mol)	Dock score (S)
EGFR	MET790C—SD	H-donor	4.21	−0.6	−6.79
(PDB id: 6JX4)	LYS745 F—NZ	H-acceptor	2.93	−2.7	
BRAF	SER536 CL—OG	H-donor	3.51	−0.5	−8.13
(PDB id: 4XV2)	PHE595 O—N	H-acceptor	3.14	−2.8	
	VAL471 5-ring—CG2	pi-H	3.85	−0.6	

Table 5
Substructural features of the inhibitor.

Molecule	Number of groups of NH	Number of Fluorine	Number of groups of C═O	Number of nitrogen	Number of 6-Ring	Number of 6-Ring (5C1N)	Number of 5-Ring
LMEB−1	2	1	1	5	3	1	1

Table 6
Key functional groups for inhibitors of EGFR and BRAF targets.

Target	Number of groups of NH	Number of Fluorine	Halogen Selecting Priority	Number of functional groups of C═O	Number of nitrogens
EGFR	2–3	1–2	fluorine > chlorine > bromine	1–2	5–7
BRAF	2–3	1–2	fluorine > chlorine > bromine	1–2	5–7

5. Conclusions

The present study developed novel models for predicting the bioactivity of EGFR and BRAF inhibitors. The RF model was found to be the preferred choice for predicting the bioacitivity of EGFR and BRAF inhibitors. In addition, as far as we know, this is the first study to reveal that EGFR and BRAF inhibitors exhibit the same selecting priority of fluorine > chlorine > bromine. The molecular docking uncovers that hydrogen bond formation is a key factor affecting the priority of fluorine > chlorine > bromine. Our findings indicate that it is critical to appropriately increase the elements of chlorine or fluorine in the structures of BRAF and EGFR inhibitors.

Ethics approval

Not applicable.

Author contributions

H. L. Z.: contributed to the study design, data collection, and analysis, as well as to the writing and editing of the manuscript. **H. H. Y. T.:** contributed to the review/editing of the manuscript.

Declaration of Competing Interest

None of the authors has any conflict of interest.

References

1. World Health Organization. Lung Cancer. Published June 26, 2023. Accessed March 1, 2024. 〈https://www.who.int/news-room/fact-sheets/detail/lung-cancer〉
2. Sher T, Dy GK, Adjei AA. Small cell lung cancer. *Mayo Clin Proc.* 2008;83(3):355–367.
3. Zou J, Guo S, Xiong MT, et al. Ageing as key factor for distant metastasis patterns and prognosis in patients with extensive-stage Small Cell Lung Cancer. *J Cancer.* 2021;12(6):1575–1582.
4. Molina JR, Yang P, Cassivi SD, Schild SE, Adjei AA. Non-small cell lung cancer: epidemiology, risk factors, treatment, and survivorship. *Mayo Clin Proc.* 2008;83(5):584–594.
5. Yan W. Wistuba II, Emmert-Buck MR, Erickson HS. Squamous Cell Carcinoma - Similarities and Differences among Anatomical Sites. *Am J Cancer Res.* 2011;1(3):275–300.
6. Schuler M, Wu YL, Hirsh V, et al. First-Line Afatinib versus Chemotherapy in Patients with Non-Small Cell Lung Cancer and Common Epidermal Growth Factor Receptor Gene Mutations and Brain Metastases. *J Thorac Oncol.* 2016;11(3):380–390.
7. Chen YY, Chang SC, Chang CY, et al. Real-world effectiveness of second-line Afatinib versus chemotherapy for the treatment of advanced lung squamous cell carcinoma in immunotherapy-naïve patients. *BMC Cancer.* 2021;21(1):1225.
8. Zhong WZ, Yan HH, Chen KN, et al. Erlotinib versus gemcitabine plus cisplatin as neoadjuvant treatment of stage IIIA-N2 EGFR-mutant non-small-cell lung cancer: final overall survival analysis of the EMERGING-CTONG 1103 randomised phase II trial. *Signal Transduct Target Ther.* 2023;8(1):76.

9. Miura S, Yamanaka T, Kato T, et al. Treatment Rationale and Design of a Phase III Study of Afatinib or Chemotherapy in Patients with Non-small-cell Lung Cancer Harboring Sensitizing Uncommon Epidermal Growth Factor Receptor Mutations (ACHILLES/TORG1834). *Clin Lung Cancer.* 2020;21(6):e592–e596.
10. Herbst RS. Review of epidermal growth factor receptor biology. *Int J Radiat Oncol Biol Phys.* 2004;59(2):21–26 Suppl.
11. Singh M, Jadhav HR. Targeting non-small cell lung cancer with small-molecule EGFR tyrosine kinase inhibitors. *Drug Discov Today.* 2018;23(3):745–753.
12. Zhang Y, Sheng J, Kang S, et al. Patients with exon 19 deletion were associated with longer progression-free survival compared to those with L858R mutation after first-line EGFR-TKIs for advanced non-small cell lung cancer: a meta-analysis. *PLoS One.* 2014;9(9):e107161.
13. Gazdar AF. Activating and resistance mutations of EGFR in non-small-cell lung cancer: role in clinical response to EGFR tyrosine kinase inhibitors. *Oncogene.* 2009;28(1):S24–S31 Suppl 1.
14. Asai N, Ohkuni Y, Yamaguchi E, Kaneko N. Successful treatment of non-small cell lung cancer with gefitinib after erlotinib-induced severe eyelid erosion: Two case reports. *J Cancer Res Ther.* 2015;11(3):653.
15. Kunimasa K, Yoshioka H, Iwasaku M, et al. Successful treatment of non-small cell lung cancer with gefitinib after severe erlotinib-related hepatotoxicity. *Intern Med.* 2012;51(4):431–434.
16. Chen D, Song Z, Cheng G. Clinical efficacy of first-generation EGFR-TKIs in patients with advanced non-small-cell lung cancer harboring EGFR exon 20 mutations. *Onco Targets Ther.* 2016;9:4181–4186.
17. Ma C, Wei S, Song Y. T790M and acquired resistance of EGFR TKI: a literature review of clinical reports. *J Thorac Dis.* 2011;3(1):10–18.
18. Yun CH, Mengwasser KE, Toms AV, et al. The T790M mutation in EGFR kinase causes drug resistance by increasing the affinity for ATP. *Proc Natl Acad Sci U S A.* 2008;105(6):2070–2075.
19. Lavoie H, Therrien M. Regulation of RAF protein kinases in ERK signalling. *Nat Rev Mol Cell Biol.* 2015;16(5):281–298.
20. Sithanandam G, Kolch W, Duh FM, Rapp UR. Complete coding sequence of a human B-raf cDNA and detection of B-raf protein kinase with isozyme specific antibodies. *Oncogene.* 1990;5(12):1775–1780.
21. Sithanandam G, Druck T, Cannizzaro LA, Leuzzi G, Huebner K, Rapp UR. B-raf and a B-raf pseudogene are located on 7q in man. *Oncogene.* 1992;7(4):795–799.
22. Hannan EJ, O'Leary DP, MacNally SP, et al. The significance of BRAF V600E mutation status discordance between primary cutaneous melanoma and brain metastases: The implications for BRAF inhibitor therapy. *Medicine (Baltimore).* 2017;96(48):e8404.
23. Ottaviano M, Giunta EF, Tortora M, et al. BRAF Gene and Melanoma: Back to the Future. *Int J Mol Sci.* 2021;22(7):3474.
24. Leonetti A, Facchinetti F, Rossi G, et al. BRAF in non-small cell lung cancer (NSCLC): Pickaxing another brick in the wall. *Cancer Treat Rev.* 2018;66:82–94.
25. De Luca A, Carotenuto A, Rachiglio A, et al. The role of the EGFR signaling in tumor microenvironment. *J Cell Physiol.* 2008;214(3):559–567.
26. Cohen C, Zavala-Pompa A, Sequeira JH, et al. Mitogen-actived protein kinase activation is an early event in melanoma progression. *Clin Cancer Res.* 2002;8(12):3728–3733.
27. Mosesson Y, Yarden Y. Oncogenic growth factor receptors: implications for signal transduction therapy. *Semin Cancer Biol.* 2004;14(4):262–270.
28. Wan PT, Garnett MJ, Roe SM, et al. Mechanism of activation of the RAF-ERK signaling pathway by oncogenic mutations of B-RAF. *Cell.* 2004;116(6):855–867.
29. ChEMBL Database. EBI. Updated 2023. Accessed March 1, 2024. ⟨https://www.ebi.ac.uk/chembl/⟩.
30. DrugBank. Contact Sales. Accessed March 1, 2024. ⟨https://www.drugbank.com/contact/sales?ref=www.drugbank.com%2Fuse_cases%2Fml-drug-discovery-repurposing⟩
31. Breiman L. Random Forests. *Mach Learn.* 2001;45:5–32.
32. Gao E. A Deep Learning Approach to Predicting Bioactivity of Small Molecules Based on Molecular Structure. Accessed March 1, 2024. ⟨https://cs230.stanford.edu/projects_fall_2021/reports/102964807.pdf⟩
33. Dhanve P, Aggarwal P, Choure S, Dhaked DK, Banerjee S. Ambroxol: A potential therapeutics against neurodegeneration. *Health Sci Rev.* 2023;7:100096.
34. Afrooghe A, Babaei M, Shayan M, Ahmadi E, Mohammad Jafari R, Dehpour AR. Therapeutic potential of bromhexine for acute itch in mice: Involvement of TMPRSS2 and kynurenine pathway. *Int Immunopharmacol.* 2023;117:109919.
35. Petrelli A, Valabrega G. Multitarget drugs: the present and the future of cancer therapy. *Expert Opin Pharmacother.* 2009;10(4):589–600.